Multiple Foci in Parietal and Frontal Cortex Activated by Rubbing Embossed Grating Patterns Across Fingerpads: A Positron Emission Tomography Study in Humans

Harold Burton,[1] Ann-Mary K. MacLeod,[2] Tom O. Videen[2,3] and Marcus E. Raichle[2,3,4]

[1]Department of Anatomy and Neurobiology, [2]Department of Radiology, Division of Radiological Sciences, [3]Department of Neurology and Neurological Surgery, Mallinckrodt Institute of Radiology, [4]The McDonnell Center for the Study of Higher Brain Function, Washington University School of Medicine, St Louis, MO 63110, USA

Somatosensory representations occupy parietal postcentral gyral (S1) and lateral sulcal-opercular cortex (S2). To address the issue of possible multiple activation foci in these regions and possible differences due to stimulating skin directly or through an imposed tool, we studied changes in cerebral blood flow with positron emission tomography during passive tactile stimulation of one or two fingertips. Restrained fingers were rubbed with embossed gratings using a rotating drum stimulator in 11 subjects. For different scans, gratings touched the skin directly for optimal stimulation of cutaneous receptors (called skin mode stimulation) or indirectly through an imposed guitar plectrum snugly fitted to the same fingers (called tool mode stimulation). The latter was expected to stimulate deep receptors better. Subjects estimated roughness after each scan. Direct skin contact activated statistically validated foci in both hemispheres. On the contralateral side these foci occurred in the anterior and posterior limbs of the postcentral gyrus and on the ipsilateral side only in the posterior limb. Tool mode stimulation activated one contralateral focus that was in the posterior limb of the postcentral gyrus. These results suggest at least two maps for distal fingertips in S1 with the anterior and posterior foci corresponding, respectively, to activations in area 3b and the junction between areas 1 and 2. In contralateral S2, skin mode stimulation activated a peak that was anterior and medial to a focus associated with tool mode stimulation. The magnitude of PET counts contralateral to stimulation was greater in the anterior S1 and the S2 regions during initial scans but reversed to more activation in the posterior S1 during later scans. These short-term practice effects suggest changes in neural activity with stimulus novelty.

Introduction

An extensive literature (of which only representative citations are presented) shows corresponding anatomical and functional divisions of the postcentral gyrus in primates (Brodmann, 1903, 1905; Campbell, 1905; Economo, 1929; Powell and Mountcastle, 1959; Paul *et al.*, 1972; Kaas *et al.*, 1979; Jones and Porter, 1980; Jones and Friedman, 1982; Jones, 1985; Iwamura *et al.*, 1993). From anterior to posterior these are areas 3a, 3b, 1 and 2. In monkeys each area possibly contains one complete body map (Nelson *et al.*, 1980; Pons *et al.*, 1985, 1987). In addition, representations for the fingertips point anterior in area 3b, posterior in area 1 and anterior again in area 2. Cells in areas 3b and 1 display characteristic predominant responsiveness to stimulation of cutaneous receptors; cells in areas 3a and 2 are more sensitive to stimulation of deep receptors (Powell and Mountcastle, 1959; Iwamura *et al.*, 1993). Hypothetically, analogous multiple maps exist in humans. Thus, two or more representations of the fingertips should exist sagittally across the postcentral gyrus. Furthermore, these separate activation foci might be distinguishable in positron emission tomography (PET) images as the average distance between the posterior bank of the central sulcus and anterior bank of the postcentral sulcus in the finger region exceeds 10 mm and is therefore resolvable with current image resolution limits (Talairach and Tournoux, 1988; Damasio, 1995). Cytoarchitectonic studies show that 3b and the junction between areas 1 and 2 occupy these two anatomically distinguishable regions (Brodmann, 1903; Economo, 1929). This suggests that the location of activation foci across the postcentral gyrus might overlay these cytoarchitectonic divisions. Previous neuroimaging studies have mainly described a single focus in peri-Rolandic cortex (Okada *et al.*, 1984; Fox *et al.*, 1987; Roland and Seitz, 1991; Suk *et al.*, 1991; Seitz and Roland, 1992a; Roland, 1993; Forss *et al.*, 1994; Hammeke *et al.*, 1994; Mogilner *et al.*, 1994; Puce *et al.*, 1995) whose location shifted with stimulation sites, i.e. medial, lower limb; and lateral, face areas (Fox *et al.*, 1987); or digits 5 to 1 sequentially from medial to lateral in the middle of the gyrus (Baumgartner *et al.*, 1991). There have been no reports of separate anterior and posterior foci across the postcentral gyrus using activation with passive somatosensory stimulation.

Parietal opercular cortex in monkeys also contains multiple somatosensory areas (Jones and Powell, 1970; Robinson and Burton, 1980b; Hyvärinen, 1982; Jones, 1985; Burton, 1986; Burton *et al.*, 1995; Krubitzer *et al.*, 1995). Two regions have relatively complete maps of the body that include enlarged hand representations (Burton *et al.*, 1995; Krubitzer *et al.*, 1995). The more anterior region has stronger connections with area 3b (Krubitzer *et al.*, 1993; Burton *et al.*, 1995) and may be more responsive to cutaneous stimulation (Robinson and Burton, 1980c). Neuroimaging studies in humans have reported somatosensory activation foci on the parietal operculum and insula (Hari *et al.*, 1983; Seitz and Roland, 1992a; Burton *et al.*, 1993; Hari *et al.*, 1993; Casey *et al.*, 1994; Coghill *et al.*, 1994; Ledberg *et al.*, 1995). Speculations about analogous sites across species are questionable because stimulation protocols differed considerably between studies. Theoretically, the fingertips should be represented multiply along the human parietal operculum if its organization resembles the pattern in monkeys.

Using PET scans, we assessed the number and distribution of cortical regions activated by rubbing textured surfaces across one or two fingertips. Controlled stimulation was applied passively to restrained fingers as has been done previously in monkeys using similar surface patterns (Darian-Smith *et al.*, 1984). Surface contact was in two modes: directly against the skin or indirectly through an imposed tool (plectrum). The first mode optimally stimulated cutaneous receptors as the gratings rubbed against the skin. It has been suggested that sensations of surfaces touched with rigid objects are transmitted through stimulation of Pacinian corpuscles (Johnson and Hsiao, 1992) and possibly muscle spindles. These two modes of stimulation might therefore distinguish somatosensory cortex foci for cutaneous versus deep receptors. Using a repeated measures design, subjects were scanned four times with each stimulation mode. This reduced noise in the averaged images and allowed

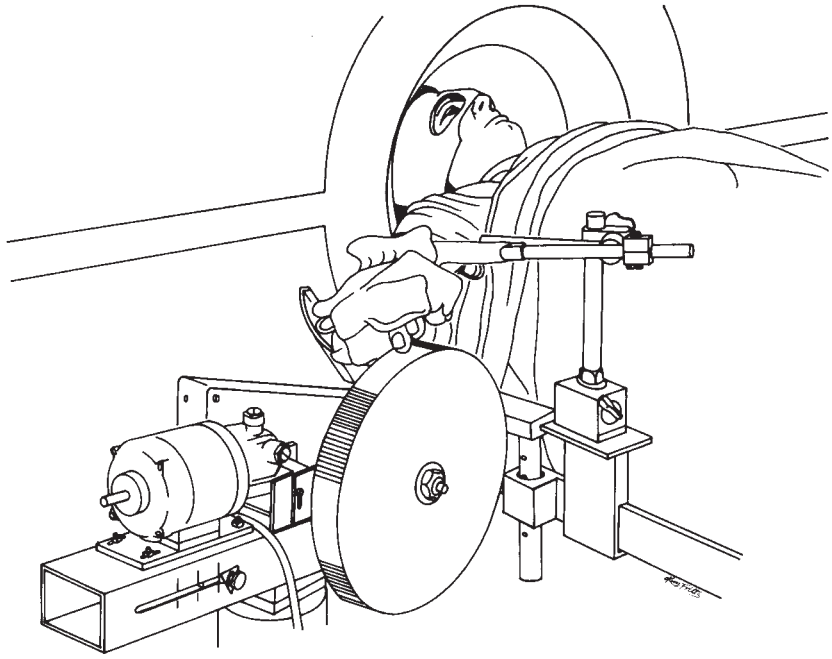

Figure 1. Stimulator and hand restraint system. See description in Materials and Methods.

cross-validation statistical testing of observed foci. The results showed activation foci in four or five parietal cortex regions.

Materials and Methods

Subjects

Paid volunteers came from the local population of students and staff at Washington University. Eleven neurologically and psychologically normal subjects (five males and six females) were between the ages of 19 and 25 (mean 22.3, SD 2.24). All reported strong right-handed preference as measured by the Edinburgh Handedness Inventory (Raczkowski *et al.*, 1974). Informed consent, obtained before participation, followed guidelines approved by the Human Studies Committee and the Radioactive Drug Research Committee of Washington University.

Stimulus Application

The tactile stimulus consisted of embossed horizontal gratings, commercially prepared by photoetching polyamide sheets of plastic. The gratings were six sequential, end-to-end pairs of alternating patches (~50 mm long by 25 mm wide) of smooth and rough surfaces (0.5 and 2.75 mm groove widths). Ridge widths (0.25mm) and groove depth (~0.75mm) were constant. A continuous strip of gratings covered the perimeter of a 25 cm diameter wheel, which was rotated by a reduced-speed, high torque DC motor. The wheel was suspended against a torsion-damped counterbalance whose fulcrum could be adjusted to provide a constant force load against the finger during stimulation.

After immobilizing the head in the scanner with an individually molded plastic mask (Fox *et al.*, 1985), similar material was molded to hold the right arm and hand to a clamp, which was rigidly attached to the scanner bed. Two fingers extended through the cast where they were held slightly flexed and together by additions to the cast and by splinting with tongue depressors (Fig. 1). We instructed subjects to relax their limb and let the cast keep their fingertips aligned against the stimulator. Given differences in finger length we successfully stimulated digits 2 and 3 in seven subjects, digits 3 and 4 in one subject and digit 2 in three subjects.

Stimulation involved rotating the gratings across the distal tips of the fingers. During different scans the gratings contacted the finger directly (called skin mode) or indirectly through ring-like plectrums fitted to the same fingers (called tool mode). During control scans the hand remained in the same position but the grating surface was moved away from the fingertip. The plectrums were left on during one of the control scans. Subjects held their eyes closed during all scans. Sounds were muffled with earplugs.

For the skin mode experiment, the top of the grating-wheel was positioned below the extended fingertips and rotated across the glabrous skin in nine subjects and along the fingertip from proximal to distal in two subjects. Initial alignment and contact were with the wheel counterbalanced at zero force. Before stimulation the counterbalance weight was adjusted to raise the wheel against the fingers with a force of ~100 g. Stimulation started on average ~60 s before the scan. With a rotation speed of ~100 mm/s, 5.1 full circumferences of the wheel passed across the finger during a 40 s scan. This yielded alternating roughness changes of ~12 per revolution or ~60 per scan.

For the tool mode experiment the grating wheel surface only touched the plectrums but again with ~100 g counterbalance force. The plectrums were extensions of molded plastic rings. From amongst a variable range of ring sizes, we fitted the distal phalange so that the plectrum stayed in place without being held by the subjects. The plectrum-extension from the ring engaged the grating surface. We adjusted the axis of rotation to be more parallel to the finger for maximal engagement of the plectrum across successive gratings. Rotation direction was from proximal to distal.

Scans during different stimulation modes (four each) or controls (two) were obtained in random order with the following constraints. The first scan was always one of the stimulation modes. Scans with the same stimulation mode never followed sequentially. Control scans occurred in the third and seventh scans.

Subjects were instructed to attend to the transitions in roughness and to the magnitude of sensations produced by the gratings. Subjects scaled roughness according to their own criteria. There was no prompting or prior experience. Requests for reporting sensations served to keep the subjects vigilant during scans. Subjects reported their sensations after each scan with stimulation. Once a subject experienced each mode of stimulation they were prompted to describe any differences in sensation between the stimulation modes just received and during prior scans. We asked for subjective differences in roughness magnitude experienced with the different stimulation modes and between recent and earlier stimulation with the same mode. [Subjects were asked the following only after activation scans. (i) Describe the magnitude of the roughness you felt. (ii) Did the transitions between the surfaces feel more or less

Table 1
Cross-validation of PET counts in regions activated by skin and tool modes of stimulation

	Anatomical region[a]	Stereotaxic coordinates hypothesis generating set[b]			Stereotaxic coordinates all subtraction pairs[b]			t[c]	P[d]
		X	Y	Z	X	Y	Z		
Skin mode									
1	Posterior postcentral gyrus (contraleral)	–41	–37	46	–37	–37	48	4.90	0.0006
2	Anterior postcentral gyrus	–51	–15	42	–51	–23	46	3.00	0.0086
3	Superior parietal gyrus	–29	–63	52	–29	–63	50	1.94	0.04
4	Parietal operculum	–43	–21	20	–45	–23	20	3.17	0.0066
5	Posterior postcentral gyrus (ipsilateral)	41	–37	46	37	–37	48	2.06	0.037
6	Medial frontal	–1	5	50	–3	5	50	3.28	0.0056
Tool mode									
7	Posterior postcentral gyrus (contraleral)	–39	–35	50	–37	–39	48	7.46	0.0001
8	Precentral gyrus	–55	–15	54	–53	–15	54	2.22	0.03
9	Parietal operculum	–41	–27	24	–47	–32	30	2.90	0.01
10	Middle frontal gyrus	–39	–15	32	–39	–15	32	2.52	0.02

[a]Numbers for named anatomical regions match labeled boxes in Figures 2–6.

[b]Stereotaxic coordinates from atlas (Talairach and Tournoux, 1988) for the peak PET difference count that was >10% greater than the count in any neighboring pixel within a radius of 11 mm. Hypothesis generating data set includes one-half of all subtraction pairs.

[c]Studentized t value for testing whether magnitude of PET difference count in five-pixel diameter voxels for the hypothesis testing data set equalled zero. The volume was centered on the coordinates of the peak listed in the column for hypothesis generating data set.

[d]Probability values of t values, uncorrected for the six skin and four tool mode regions.

distinguishable from your experiences in the previous scan? (iii) Did the surfaces feel the same or different when they touched your skin directly or through the tool? They were asked to describe the differences.]

PET Scanning Techniques

Images from 31 transaxial slices, with 3.375 minimum spacing, were acquired on a Siemens 953B scanner using previously described scanning methods for tracing an intravenous bolus injection of ^{15}O-labeled water (8–10 ml of saline with ~15 mCi of radioactivity per scan) (Fox *et al.*, 1984; Fox *et al.*, 1985; Fox *et al.*, 1988; Mintun *et al.*, 1989). [In-plane pixel size was 2.086 mm^2. Counts were collected in the three-dimensional mode (septa retracted) with stationary acquisition. These data were reconstructed with a ramp filter and a filtered back-projection algorithm. The original 31 slices were interpolated to 49 slices with cubic voxel dimensions in the final image of 2 mm^3.] The images were based on counts reflecting tracer activity because regional cerebral blood flow is nearly linearly related to regional tissue radiotracer concentration in scans lasting <1 min (Fox *et al.*, 1984). As shown previously, the percentage change in regional tissue radioactivity is equivalent to the percentage change in regional blood flow for response localization in averaged subtraction images (Fox and Mintun, 1989). Before any analyses of results from different scans was performed, all images were normalized by linear scaling for global tracer activity to a value of 1000 PET counts (Fox *et al.*, 1987) and transformed to a standardized stereotaxic space using a lateral skull X-ray to estimate the AC–PC plane (Fox *et al.*, 1985; Talairach and Tournoux, 1988). Thus all regional activity measurements were placed in stereotaxic space of the atlas anatomy and not the cerebral anatomy of individual subjects (Fox *et al.*, 1985). Comparisons were therefore on a per pixel basis from stereotaxically matched locations. Image pairs of each activation minus control scan for each subject were screened for excessive head movements between scans. Individual difference images with head movements of <1.5 mm were used in further analyses. Difference images were passed through a three-dimensional, fifth-order, low-pass Butterworth filter with a cut-off frequency of 7 cycles/cm. This last step produced an image with a resolution of ~11 mm FWHM in all dimensions.

Statistical Methods

We used an objective method to evaluate the significance of increased regional blood flow foci observed in the averaged summed difference images. This involved cross-validation procedures between two equal halves of the data obtained from a stimulation mode (Squire *et al.*, 1992; Burton *et al.*, 1993; Drevets *et al.*, 1995; Houton *et al.*, 1996). First, for each subject we selected up to four subtraction pairs (e.g. activation–control) that included each of the activation scans for both controls. Two subtraction pairs from either the first or last activation scans were randomly assigned to a *hypothesis generating* or *hypothesis testing* data set. Next, the subtraction pairs from the hypothesis generating set were averaged using proportional weighting to balance contributions from each subject to a total value of 1 in the averaged images. [The weight given to each difference image was 1 divided by the number of difference images obtained for a stimulation mode from a subject. Thus the weights varied from 0.25 to 1 (1/4 to 1/1) depending on how many activation minus control scan pairs were available from a subject. For each difference image, the difference PET count per pixel was multiplied by the weight factor before adding to the summed difference count for that pixel. The average difference count per pixel was this summed difference count divided by the number of subjects.] A computerized search of this averaged difference image identified the location of peak PET counts in a single voxel (8 mm^3) with tracer activity >10% of neighboring pixels and separated from adjacent peaks by at least 11 mm. The stereotaxic location from the top 20 maxima then established the centers for five-pixel diameter voxels (e.g. 648 mm^3). Total counts from matching locations within these volumes on the individual difference images from the remaining, hypothesis testing half of the data (again weighted by subject contributions) were assessed with a one-sample, upper-tail Student's t-test against the null hypothesis of 0 counts. Mean PET counts in the defined volumes whose t values exceeded null hypothesis expectations with a $P < 0.05$ (uncorrected) were considered significant replicates of the focal peaks identified from searching the hypothesis generating half of the data. Finally, to obtain the best approximation for the stereotaxic location of the peak responses, an average difference image was made for each stimulation mode using the combined subtraction pairs from the hypothesis generating and testing portions of the data. These data were also reweighted by total subject contributions. The coordinates of the new maxima were found with the computer search algorithm. Those located nearest the peaks used for the cross-validation testing were identified (Table 1). Individual subtraction

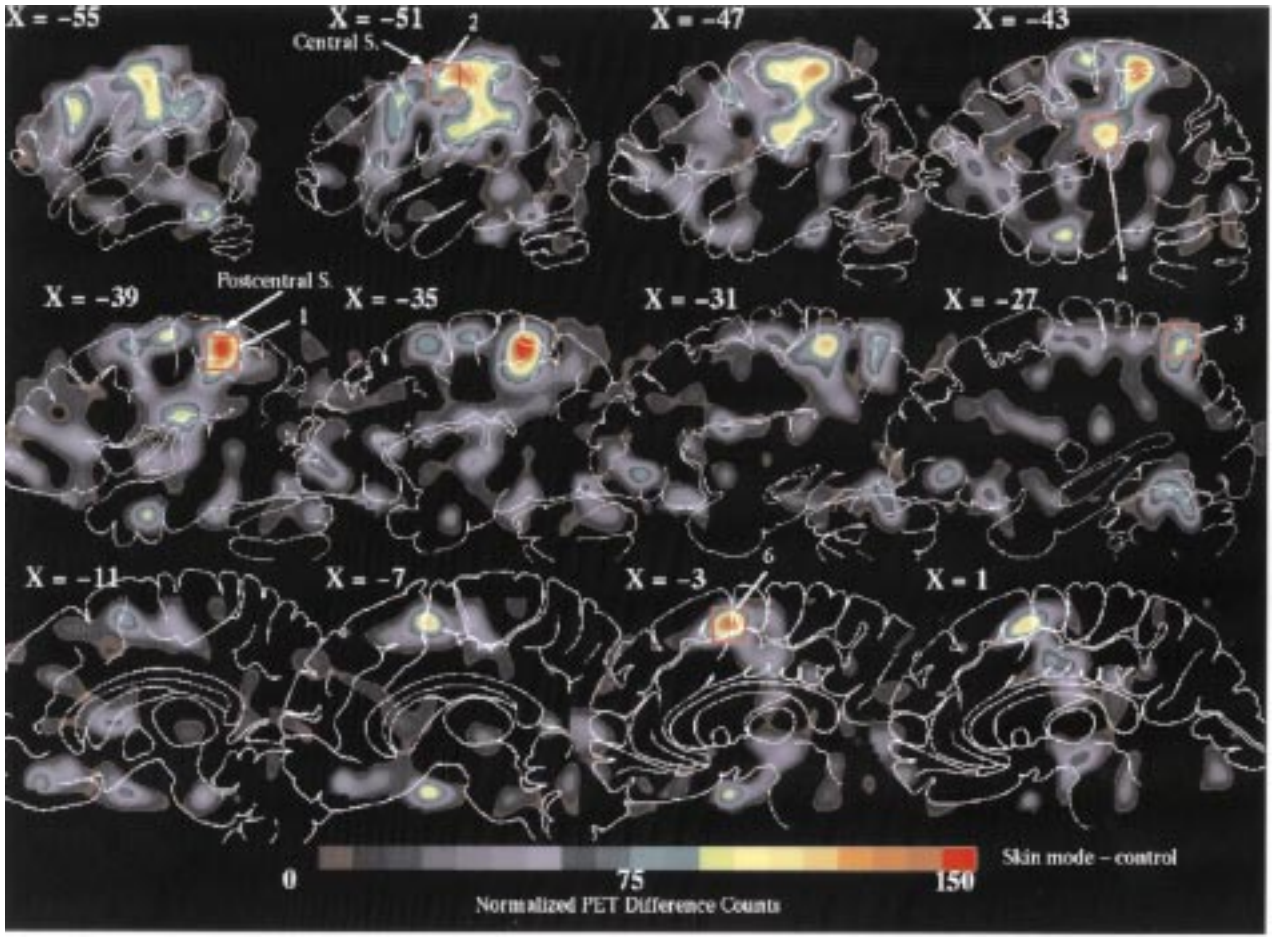

Figure 2. PET data show activation foci from skin mode stimulation on interpolated, sagittal slices at 4 mm intervals and through the left hemisphere, which was contralateral to the stimulated finger. These averaged difference images obtained from 35 subtraction pairs of scans during skin mode stimulation minus scans during no stimulation controls in nine subjects. All PET data were first normalized for global blood flows and transformed to stereotaxic space as described previously (Fox *et al.*, 1985). The color bar is scaled in units of normalized PET difference counts and, given the linear relationship between PET counts and blood flow (Fox and Mintun, 1989), reflects blood flow increases of ~1% for changes of 10 PET counts. Coordinate labels (X = ...) above each image and superimposed outline drawings of brain sections represent corresponding sagittal planes in a stereotaxic atlas (Talairach and Tournoux, 1988). Small red boxes show the central location of the peaks identified from the hypothesis generating data set (see columns 3–5 in Table 1) with skin mode stimulation in: (1) posterior postcentral gyrus, (2) anterior postcentral gyrus, (3) superior parietal gyrus, (4) parietal operculum and (6) medial frontal gyrus. The same activation foci have similar numbers in all figures and tables.

pairs were also used in statistical assessments of changes in the magnitude of regional blood flow (tracer activity) in specific regions.

We used two approaches to examine whether foci identified with the two modes of stimulation differed. The first was the issue of regional overlap in activated foci. This was tested by cross-validating between the stimulation modes. Thus the four or five regions determined to have significant PET count differences within each mode constituted the locations that defined the coordinate space to be tested in the data from scans during the other stimulation mode. For these tests, peaks were selected from the combined data from each stimulation mode whose coordinates were closest to the within mode significant foci. Thus, peaks in the combined data from skin (or tool) stimulation closely matched the cross-validated regions identified with the divided data sets for the skin (or tool) mode. The location of the closest matching peaks provided the centers of five-pixel diameter voxels to measure changes in tracer activity in the individual difference images from the other stimulation mode. Mean PET counts in the defined volumes whose t values exceeded null hypothesis expectations with a $P < 0.05$ (uncorrected) were considered significant replicates of the focal peaks identified from the other stimulation mode.

A second issue was whether the magnitude of PET count differences in identified regions for each of the modes differed. Thus the activated foci might overlap but the amount of activation varied. In nine subjects that had fully balanced data sets, a repeated measures, multivariate

Figure 3. PET data illustrate the bilateral distribution of regional blood flow changes in peri-Rolandic cortex to skin (*A*) and tool (*B*) modes of stimulation. Images are shown as averaged difference images on selected transaxial slices. The left side of the brain is shown on the left. (*A*) Images obtained from 35 subtraction pairs of scans during skin mode stimulation minus scans during no stimulation controls in nine subjects. Small white boxes show the central location of the peaks identified from the averaged difference image for all subtraction pairs with skin mode stimulation in: (1) posterior postcentral gyrus, (2) anterior postcentral gyrus, (4) parietal operculum, (5) posterior postcentral gyrus on the ipsilateral side and (6) medial frontal gyrus. (*B*) Images obtained from 32 subtraction pairs of scans during tool mode stimulation minus scans during no stimulation controls in eight subjects. Small white boxes show the central location of the peaks identified from the averaged difference image for all subtraction pairs with tool mode stimulation in: (7) posterior postcentral gyrus, (9) parietal operculum and (10) middle frontal gyrus. Grey scale in units of normalized PET difference counts. Coordinate labels (Z = ...) below each image and superimposed outline drawings of brain sections represent corresponding horizontal planes in a stereotaxic atlas (Talairach and Tournoux, 1988). The vertical lines labeled X = ... show the location of selected sagittal planes in Figures 2 and 5. The stereotaxic coordinates for the peaks in the numbered boxes are listed in columns 6–8 of Table 1. The same foci have similar numbers in all figures and tables.

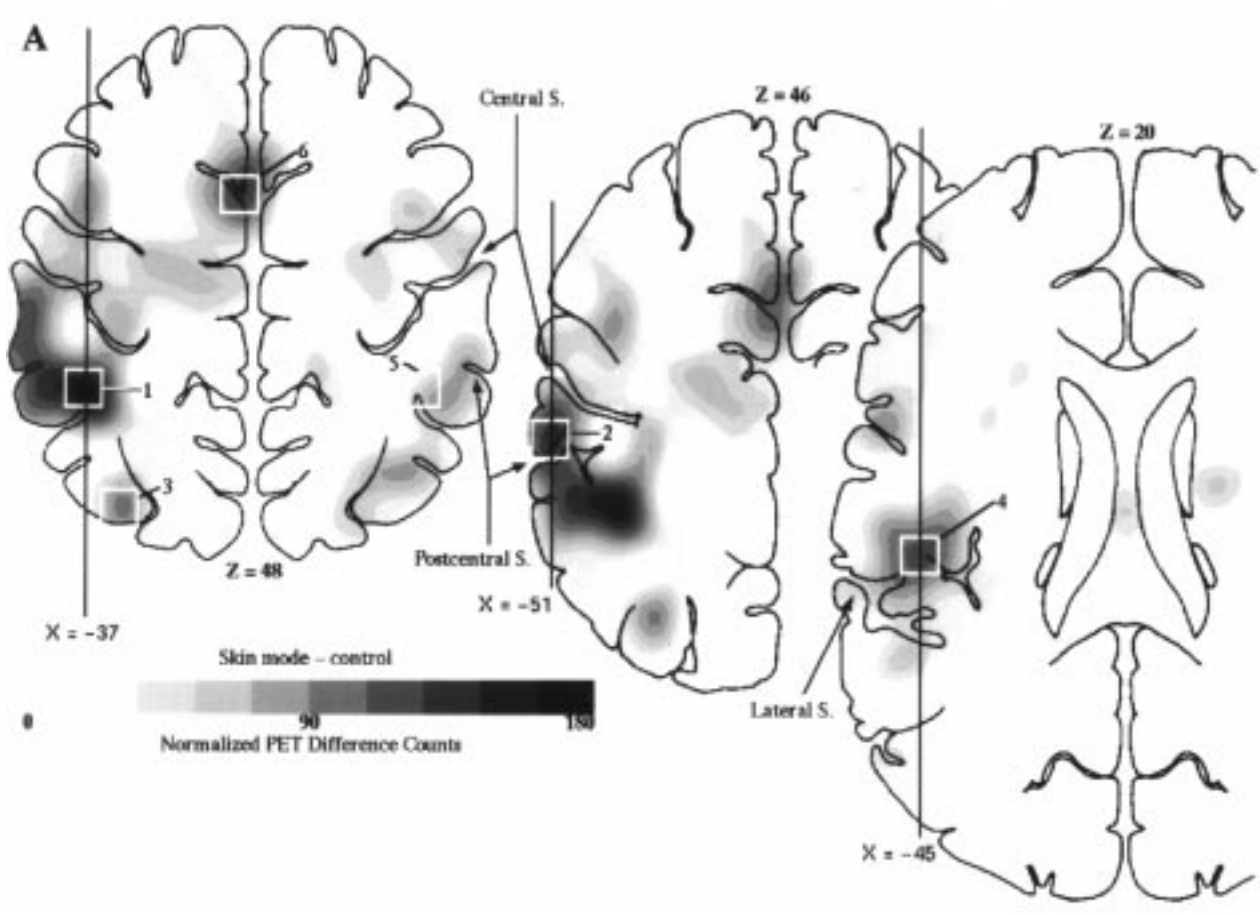
A
Central S.
Z = 46
Z = 20
1
2
3
4
5
Z = 48
Postcentral S.
X = -51
X = -37
Skin mode – control
0
90
180
Normalized PET Difference Counts
Lateral S.
X = -45

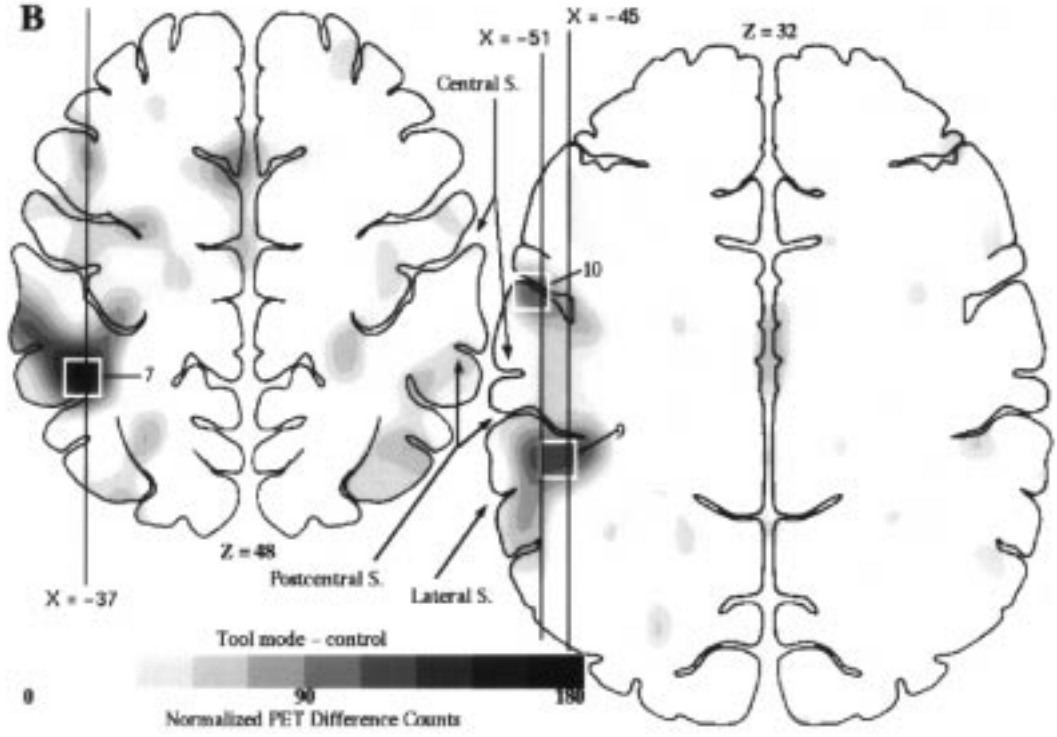
B
X = -51
X = -45
Z = 32
Central S.
10
7
9
Z = 48
Postcentral S.
Lateral S.
X = -37
Tool mode – control
0
90
180
Normalized PET Difference Counts

analysis of variance was used to examine the effects of stimulation mode (n = 2), scan number (n = 4) and subject (n = 9) on PET counts in the regions (n = 6) found significant within each stimulation mode. Counts from each subject-scan-mode included values from five-pixel diameter voxels centered on the peaks for the identified regions.

Measurements of the magnitude of PET counts in selected regions from individual subtraction pairs provided data for assessing whether the magnitude of regional blood flow changes in validated activation foci differed over time. Each subject received the same skin mode stimulation during four separate scans that occurred interspersed with six other scans consisting of two eyes-closed rest controls and four tool mode stimulation scans. As subjects had no prior experience with these stimuli, the multiple exposures across the scans included early scans when everything was novel, to later scans when the grating stimulation was familiar. Changes in PET counts per region from different scans for each subject were obtained from five-pixel diameter voxels centered on the pixel location of peak count from the combined averaged subtraction image for a statistically validated region. Difference counts from the first and last two skin mode scans were averaged and defined as early and late scan-times. For example, the early scan-time observations from a subject might include counts from scans 1 and 4 and the late scan-times might be from scans 8 and 10. The average maximum times between the first and fourth scans was ~2 h and between the second and third scans was ~0.5 h. An ANOVA model assessed average differences in PET counts in each region as the dependent variable, and the subject, region and scan-time as independent variables. The analysis used a hierarchical error term based on the subject by factor interaction (e.g. subject × scan time) to control for large variances between counts in different subjects (Keppel, 1982).

Results

The following discusses only those foci of change in regional tracer activity that cross-validated between randomly separated halves of the data.

Skin Mode Stimulation

There are five validated foci of maximal blood flow change in parietal cortex: four are contralateral (Fig. 2) and one is ipsilateral (Fig. 3*A*) to the fingertips stimulated directly with grating surfaces. In the vicinity of the postcentral gyrus the sites divide into two parts. The larger one is more posterior and occupies the anterior portion of the postcentral sulcus and adjoining postcentral gyral cortex (peak centered in box labeled 1 in Figs 2, 3*A* and Table 1) (Talairach and Tournoux, 1988). A smaller second focus lies lateral and anterior where it extends from anterior portions of the postcentral gyral cortex down into the central sulcus (peak centered in box labeled 2 in Figs 2, 3*A* and Table 1). Transaxial images (Fig. 3*A*; Z = 48 and Z = 46) clearly show two separable activated foci along coronal and sagittal planes despite the continuity of heightened changes in blood flow across this region of cortex. The more anterior focus extends sagittally over 1 cm from X = –55 to X = –43. The more posterior region is wider (~2 cm; X = –51 to X = –31). An homologous, posterior site within the postcentral sulcus also lies ipsilateral to the stimulated finger (box labeled 5 in Fig. 3*A* and Table 1).

Immediately lateral to the sites with changed blood flows in the postcentral gyrus is another focus of activation that mostly occupies buried parietal opercular cortex (peak centered in box labeled 4 in Figs 2, 3*A* and Table 1). The distribution of elevated blood flow stretches across an elongated, bilobular shaped region. Statistically only a single, anteriorly placed peak cross-validated. However, the parietal opercular activated region extends sagittally over ~1 cm (Fig. 2, slices X = –47 to X = –39). Viewing in the coronal plane shows the validated peak is more anterior and lies closer to the superior limiting sulcus than the posteriorly distributed portion of the activated region, which is more lateral and closer to the surface (Fig. 4*A*). Activated blood flow changes in the parietal operculum appear contralateral to the stimulated finger (Figs 3*A* and 4*A*).

Isolated from the preceding parietal regions is a small activated site in the vicinity of the superior parietal lobule (box labeled 3 in Figs 2, 3*A* and Table 1). This very confined focus extends sagittally ~4 mm and occurs on the side contralateral to stimulation.

One frontal cortex region contains significant increases in blood flow with direct skin stimulation. This circumscribed focus, which centers on the medial frontal gyrus (box labeled 6 in Fig. 2 and Table 1), extends sagittally ~1 cm (Fig. 2, X = –7 to X = 1). The center of activation is contralateral to the stimulus.

Tool Mode Stimulation

Eight subjects scanned during direct stimulation of the skin had additional scans during similar stimulation with grating surfaces through a tool worn on the same fingers. Tool mode of stimulation led to two validated activation foci in parietal cortex contralateral to the stimulated fingers (Fig. 5). Subtle differences distinguish the relatively similar sites activated by the two modes of stimulation. The region of maximal blood flow change for the tool mode stimulation versus control occupies the posterior limb of the postcentral gyrus. The activated region is not separated into two foci. The single region of elevated blood flow occupies an expanse whose distribution resembles the more posterior of the two regions described for skin mode stimulation (box labeled 7 in Figs 3*B*, 4*B* and 5, and Table 1). The activated region lies in the depths of the postcentral sulcus and extends anteriorly along the adjoining postcentral gyral cortex. As in the skin mode, there is a homologous region of increased blood flow ipsilateral to the stimulated finger. However, it does not reach significance in the tool mode scans (Fig. 3*B*).

Near the central sulcus on the contralateral side there is an anterior extension to the dominant activated focus (Fig. 5). However, this anterior region is not as far forward or lateral as the anterior site in the skin mode and is not detected as a separate peak within the group of scans with tool-mode stimulation. Instead, another small, validated site occupies part of the precentral gyral crown (box labeled 8 in Fig. 5 and Table 1).

The parietal operculum also shows increased blood flows with tool mode stimulation (peak centered in box labeled 9 in Figs 3*B*, 4*B* and 5 and Table 1). The center of the parietal opercular region in the tool mode is ~9 mm posterior to the

Figure 4. PET data portray regional blood flow changes in parietal opercular cortex with two modes of stimulation. Images are averaged difference images on interpolated coronal slices. The left side of the brain is shown on the left. (*A*) Images obtained from 35 subtraction pairs of scans during skin mode stimulation minus scans during no stimulation controls in nine subjects. (*B*) Images obtained from 32 subtraction pairs of scans during tool mode stimulation minus scans during no stimulation controls in eight subjects. Grey scale in units of normalized PET difference counts. Coordinate labels (Y = ...) below each image and superimposed outline drawings of brain sections represent corresponding frontal planes in a stereotaxic atlas (Talairach and Tournoux, 1988). The vertical lines labeled X = ... show the location of selected sagittal planes in Figures 2 and 5. Small white boxes show the location of the peaks identified from the averaged difference image for all subtraction pairs: (4) parietal operculum for skin mode, (7) posterior postcentral gyrus and (9) parietal operculum for tool mode stimulation. The stereotaxic coordinates for the peaks in numbered boxes are listed in columns 6–8 of Table 1. The same activated foci have similar numbers in all figures and tables.

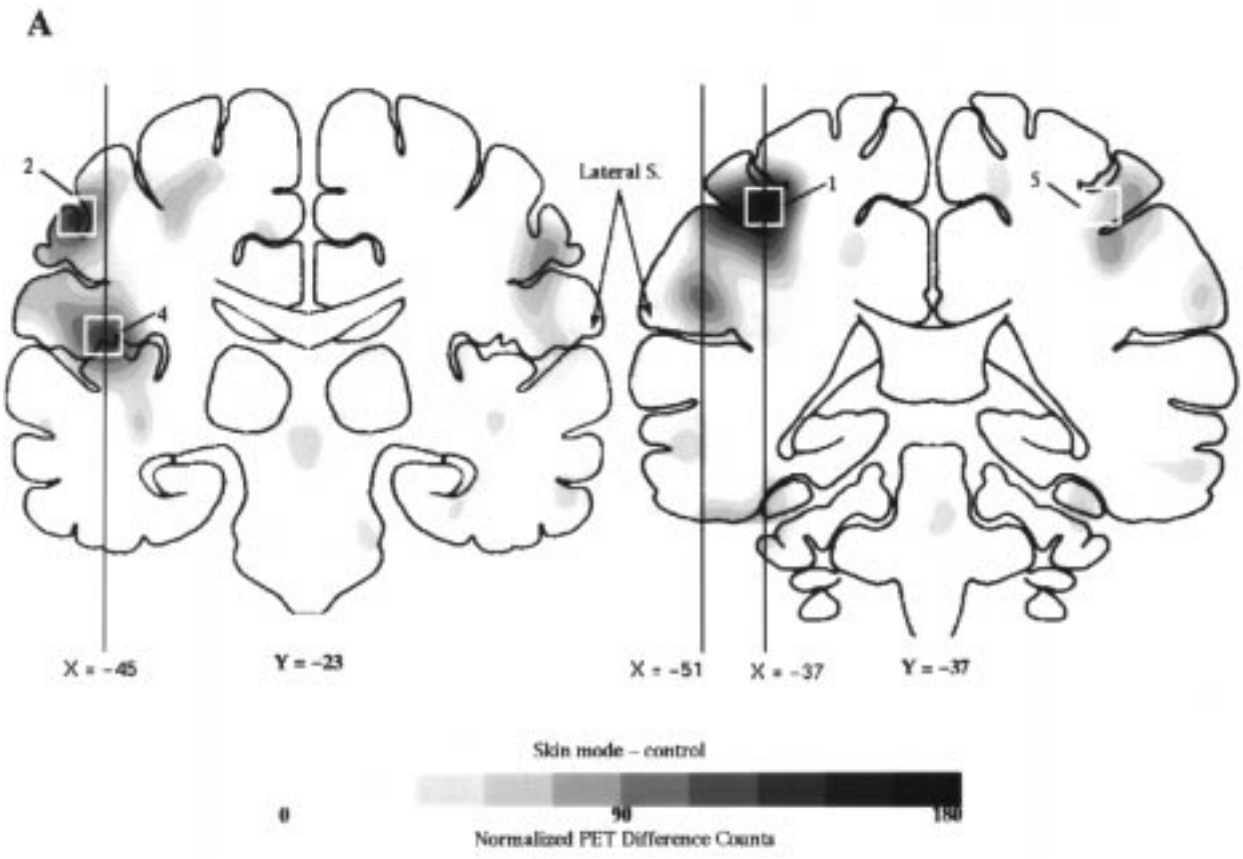
A
2
4
Lateral S.
1
5
X = -45
Y = -23
X = -51
X = -37
Y = -37
Skin mode – control
0
90
180
Normalized PET Difference Counts

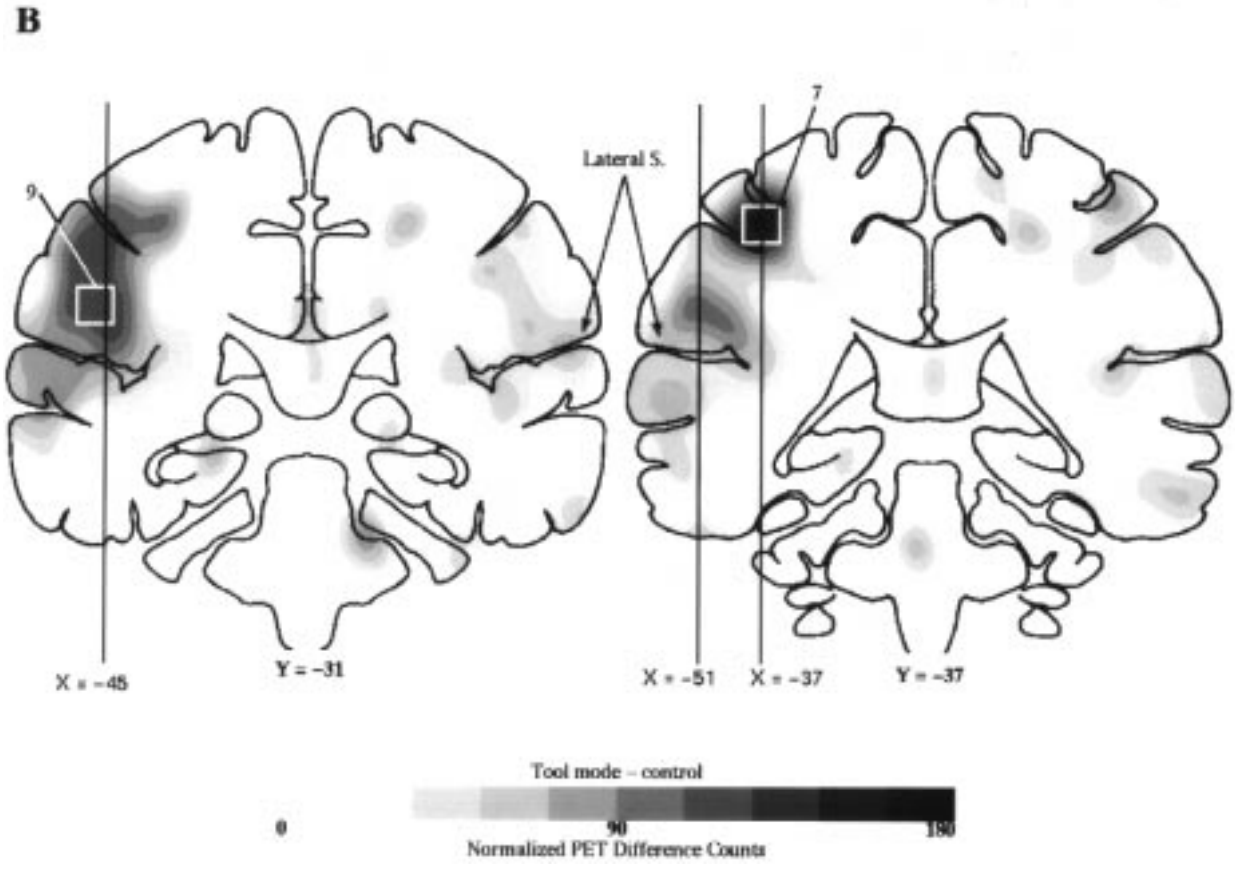
B
9
Lateral S.
7
X = -45
Y = -31
X = -51
X = -37
Y = -37
Tool mode – control
0
90
180
Normalized PET Difference Counts

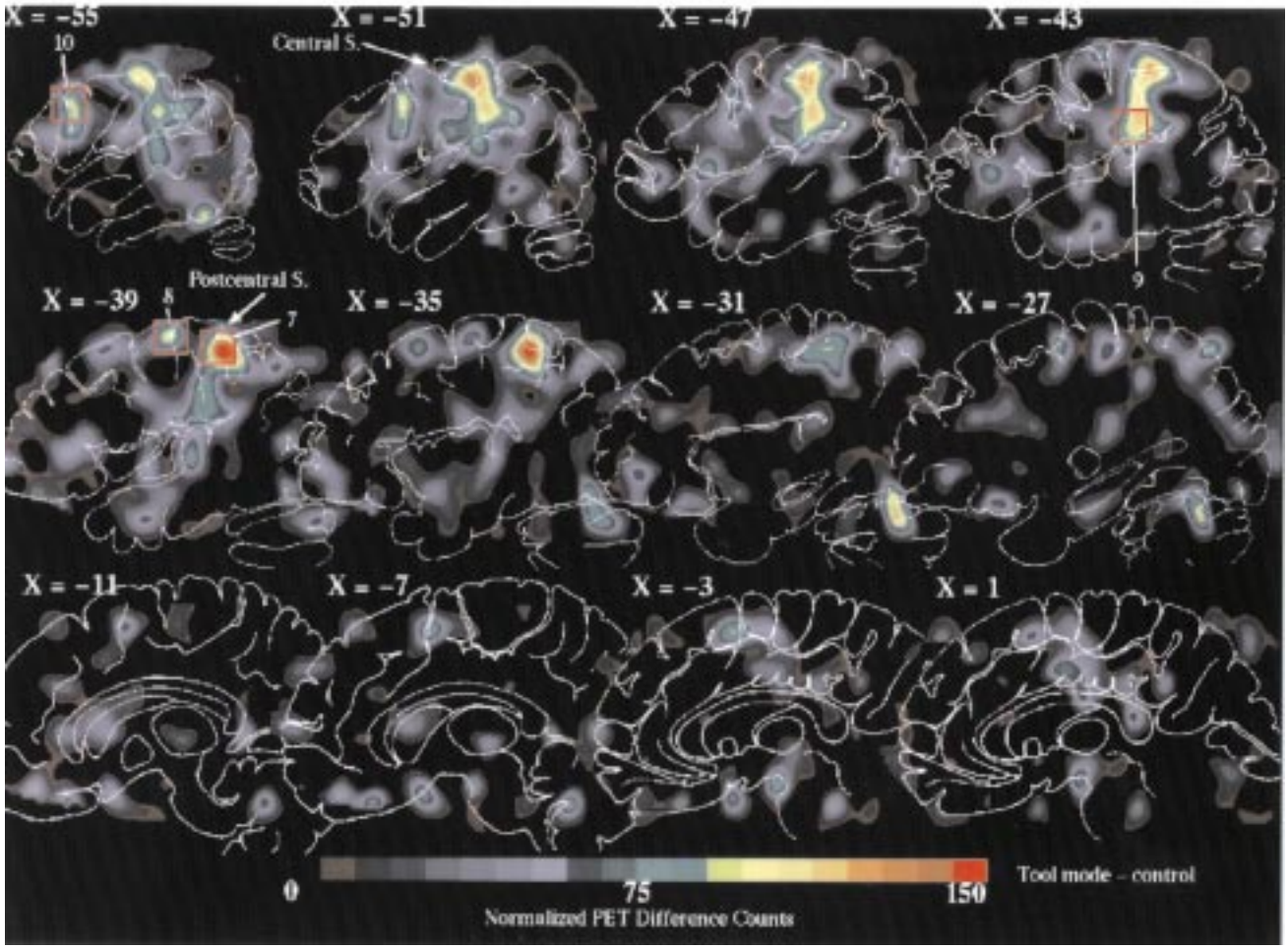

Figure 5. PET data show activation foci from tool mode stimulation on interpolated, sagittal slices at 4 mm intervals and through the left hemisphere, which was contralateral to the stimulated finger. These averaged difference images obtained from 32 subtraction pairs of scans during tool mode stimulation minus scans during no stimulation controls in eight subjects. Small red boxes show the location of the peaks identified from the hypothesis generating data set (see columns 3–5 of Table 1) with tool mode stimulation in: (7) posterior postcentral gyrus, (8) precentral gyrus, (9) parietal operculum and (10) middle frontal gyrus. The same activated foci have similar numbers in all figures and tables. See text of Figure 2 for labeling conventions and explanations.

center of the peak blood flow change for the skin mode (Fig. 4; Y = −32 for tool versus Y = −23 for skin, i.e. boxes labeled 9 versus 4). As in the skin mode, there is no activation in the vicinity of the parietal operculum on the ipsilateral side.

Two frontal cortex regions contain increases in blood flow in the tool mode. As in the skin mode, there is a change in the vicinity of the medial frontal gyrus; however, it does not reach significance in the tool mode. Additionally there is a significant activated region in the middle frontal gyrus (box labeled 10 in Figs 3*B*, 5 and Table 1). A similar activated site occupies the same part of frontal cortex with direct skin stimulation (Fig. 2) but is too small to pass our cross-validation criteria.

Overlapping Regions with Different Stimulation Modes

Statistical assessments of overlapping regional distributions of activation were obtained by cross-validation tests between stimulation modes. In these tests we used the coordinates of the peaks from validated foci within a mode to obtain the center of five-pixel diameter voxels in the data set obtained from the other stimulation mode where PET difference counts were subjected to single *t*-tests (see Materials and Methods). We also examined whether the magnitudes of mean PET difference counts for a site varied with stimulation mode. All of the validated foci identified within a mode, except the site in the superior parietal gyrus activated with skin mode stimulation, cross-validated against the other mode. This shows that the regional distribution of significantly increased blood flow overlapped with the different stimulation modes. Thus, the regional increase in blood flow identified with skin mode stimulation near the posterior limb of the postcentral gyrus (box labeled 1 in Fig. 3*A*) also had significantly greater than zero blood flow increases with tool mode stimulation in the voxel location defined by skin mode

Figure 6. PET data from skin stimulation mode show changes in magnitude of activation in various foci for different scan times. (*A*) Selected transaxial images show average difference images from 16 subtraction pairs (skin stimulation minus controls) obtained in nine subjects during the first two scans with skin mode stimulation (early). (*B*) Selected transaxial images show average difference images from 17 subtraction pairs obtained in nine subjects during last two scans with skin mode stimulation (late). PET difference counts were higher during early scans in anterior parts of the postcentral gyrus and parietal operculum (white boxes labeled 2 and 4 respectively) and were significantly higher during later scans in contralateral posterior parts of the postcentral gyrus (box labeled 1). See text of Figure 2 for labeling conventions and explanations.

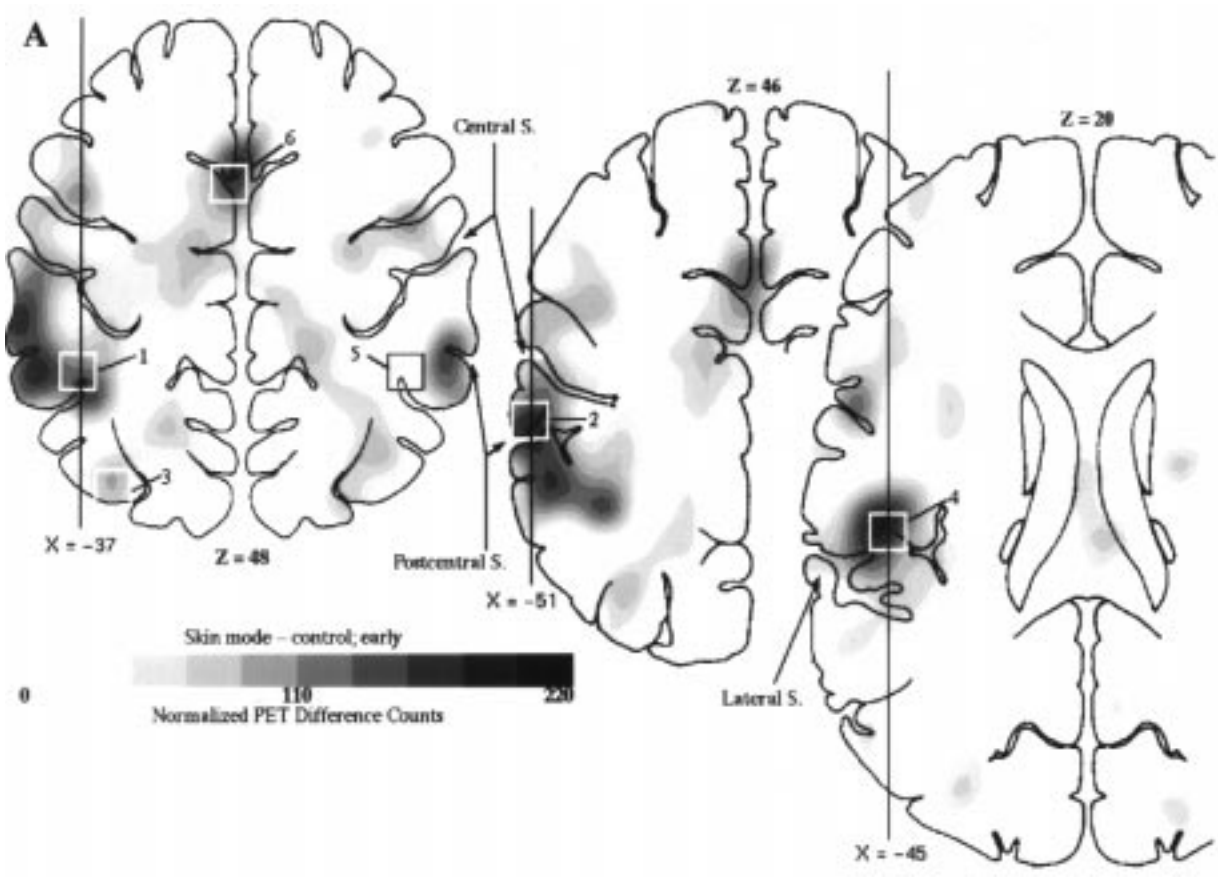
A
Z = 46
Central S.
Z = 20
6
1
5
2
3
4
X = -37
Z = 48
Postcentral S.
X = -51
Skin mode – control; early
0
110
220
Normalized PET Difference Counts
Lateral S.
X = -45

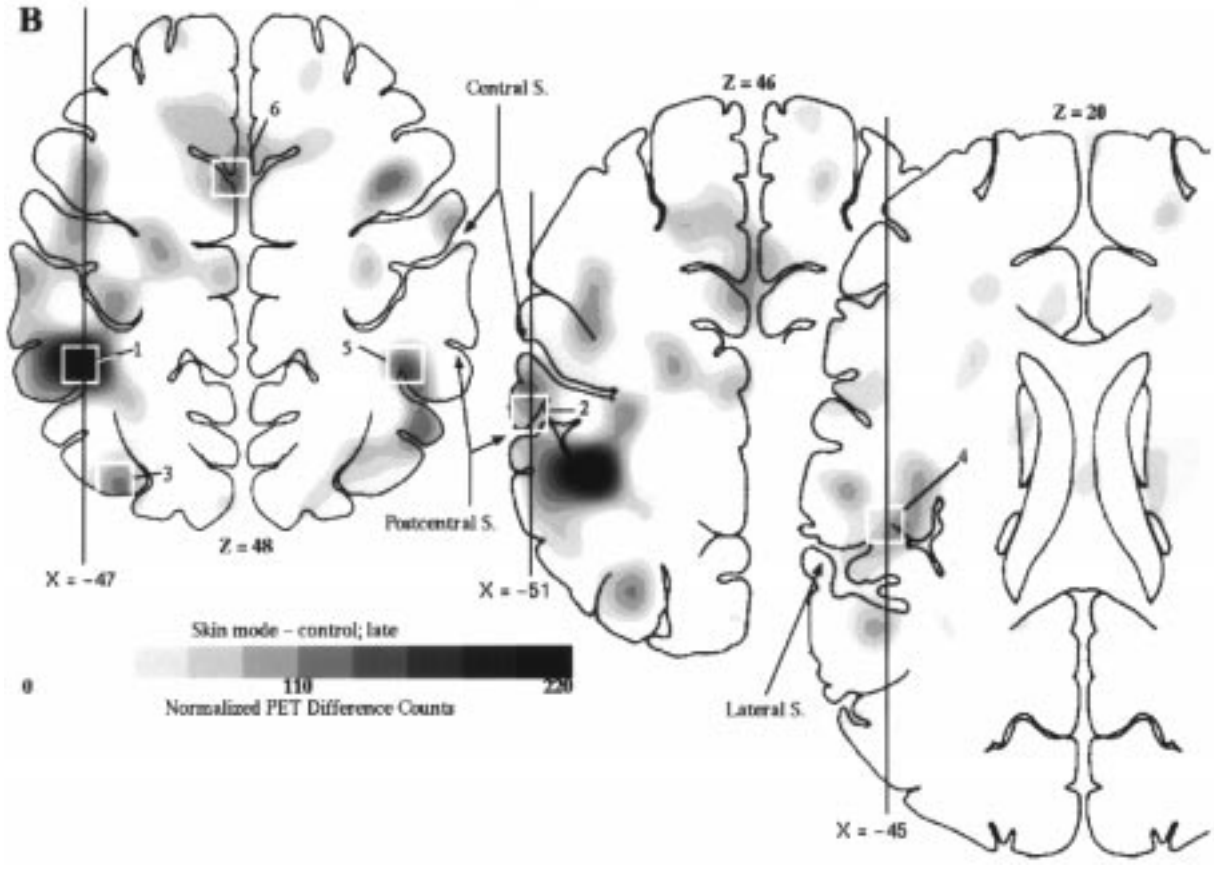
B
Central S.
Z = 46
Z = 20
6
1
5
2
3
4
Postcentral S.
Z = 48
X = -47
X = -51
Skin mode – control; late
0
110
220
Normalized PET Difference Counts
Lateral S.
X = -45

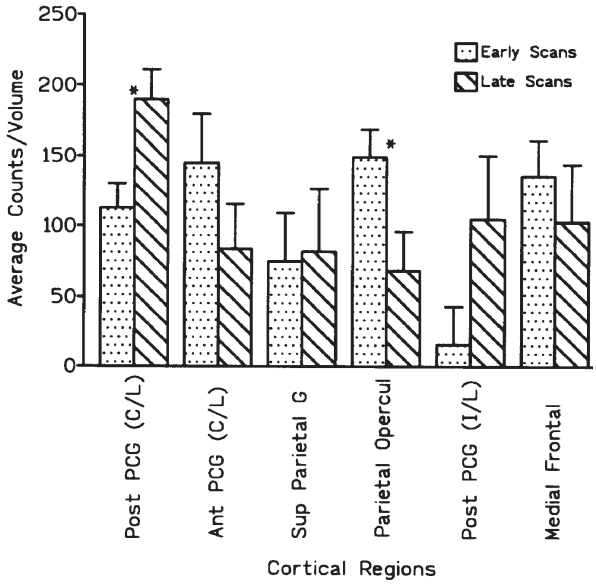

Figure 7. Bar graph shows average PET difference counts at different scan times in five-pixel diameter voxels that surrounded the peak blood flow changes in validated activation foci with skin mode stimulation. Foci listed from left to right correspond in order to boxes and rows labeled 1–6 in, respectively Figures 2, 3*A*, 4*A* and Table 2. Results are from nine subjects. Data labeled Early shows average from first two and that labeled Late from last two scans. Abbreviations: anterior postcentral gyrus, Ant PCG; contralateral, C/L; ipsilateral, I/L; parietal operculum, Parietal Opercul; posterior postcentral gyrus, Post PCG; superior parietal gyrus, Sup Parietal G.

scans (t = 6.78, P < 0.0001). Similarly, the peak identified in tool mode stimulation in the posterior limb of the postcentral gyrus (box labeled 7 in Fig. 3*B*) predicted a significant change in blood flow in the volume surrounding this peak in the skin mode scans (t = 8.43, P < 0.0001). Finding overlapping activation foci with different stimulation modes around the postcentral sulcus is not too surprising as the coordinates of activated peak blood flow changes determined for each stimulation mode are nearly identical for this location (e.g. skin mode, X = –37, Y = –37, Z = 48; tool mode, X = –37, Y = –39, Z = 48). Mean PET difference counts over these regions also did not differ between modes.

Cross-validations also occurred for the more anterior foci in peri-Rolandic cortex. The peak associated with the anterior limb of the postcentral gyrus identified with skin mode stimulation (box labeled 2 in Fig. 3*A*) predicts a significant blood flow increase centered in the same coordinate space with the tool mode (t = 4.298, P < 0.0018). Similarly, the coordinates of the anterior but non-contiguous peak in the precentral gyrus observed with tool stimulation (box labeled 8 in Fig. 3*B*) predicts a blood flow increase in the same space with the skin mode (t = 4.041, P < 0.0019). The mean PET difference count was slightly higher with skin mode stimulation over the anterior limb of the postcentral [box labeled 2 in Fig. 3*A*; F(8,1) = 4.63, P = 0.0445] but not different between modes in the precentral gyrus.

In some instances a site that cross-validated only within one stimulation mode still predicted significant blood flow changes for the other mode in data averaged from all subtraction pairs. For example, there was no cross-validation for a peak identified over the medial frontal region in the test set of scans for tool mode, but the coordinate space specified from the skin mode (box labeled 6 in Fig. 3*A*) predicted a blood flow increase in the same location for tool mode (t = 3.201, P < 0.0075). Similarly, a

Table 2
PET counts compared across time for different cortical regions

Anatomical region[a]		Peak coordinates summed set			Early/late	F(1,8)	*P*
		X	Y	Z			
1	Posterior postcentral gyrus (contralateral)	–37	–37	48	112.5/190	11.85	0.009
2	Anterior postcentral gyrus	–51	–23	46	145/84	2.05	0.19
3	Superior parietal gyrus	–29	–63	50	75/82	0.01	0.92
4	Parietal operculum	–45	–23	20	149/68	8.63	0.002
5	Posterior postcentral gyrus (ipsilateral)	37	–37	48	16/105	2.57	0.15
6	Medial frontal	–3	5	50	135/103	0.51	0.49

[a]Numbers for named anatomical regions match labeled boxes in figures.

validated peak over the middle frontal area from tool mode stimulation (box labeled 10 in Fig. 5) predicted a blood flow increase in the skin mode (t = 3.601, P = 0.0035).

In the parietal operculum the foci identified with each mode (boxes labeled 4 and 9 in Fig. 4) cross-validated against the other despite the distance between the peaks from each mode. The coordinates for the peaks from within the full data sets for each stimulation mode (e.g. skin X = –45, Y = –23, Z = 20 versus tool X = –47, Y = –32, Z = 30) are separated by ~14 mm (computed as a vector distance between coordinates). This suggests two distinguishable foci with that from the skin mode anterior to the predominant region of blood flow change from the tool mode (Fig. 4; compare boxes labeled 4 and 9 in Figs 2 and 5 respectively). Cross-validation between the modes statistically predict overlapping regions since the parietal opercular activated region is extensive in both skin and tool modes (e.g. skin mode predicts a blood flow increase in the tool mode: t = 2.918, P = 0.0112; tool mode predicts a blood flow increase in the skin mode: t = 3.954, P = 0.0021). However, there is a significant difference in the mean magnitude of PET difference counts between these two regions with different modes [F(8,1) = 8.22, P = 0.0241]. The mean PET difference counts are considerably higher with skin mode stimulation (105.2) than counts over the same more anterior region during tool mode stimulation (73.12; *post hoc* t-test P < 0.05). The mean PET difference counts are the same for the two stimulation modes over the more posterior tool mode identified peak.

Changes in PET Counts with Scan Repetitions

Because scan sessions spanned initial and late stage familiarity with the tasks, we compared the magnitudes of blood flow changes in each of the validated regions in early versus late scans for the skin mode stimulation. The results from averages obtained from two early versus two later scans show significant changes in average difference-counts and these varied by region (Figs 6, 7 and Table 2). In parietal cortex contralateral to the stimulated fingers the difference-counts are significantly higher during early scans in the volume centered on the parietal operculum (Figs 6 and 7). A similar decline in difference-counts occurred in the vicinity of the peak located on the anterior bank of the postcentral gyrus, near the central sulcus (Fig. 7) but this trend did not reach significance. In contrast, counts were significantly higher during later scans in the volume centered on the posterior limb of the postcentral gyrus, near and within the postcentral sulcus on the side contralateral to the stimulated finger (Figs 6 and 7). A similar increase in blood flows with time occurred in the matching region on the ipsilateral side (Fig. 7).

Discussion

The present findings differ from those in prior PET studies in showing more foci and, where currently identified foci overlap with previously identified regions, the activated foci are more confined (Fox *et al.*, 1987; Seitz and Roland, 1992b; Burton *et al.*, 1993; Roland, 1993; Coghill *et al.*, 1994; Ledberg *et al.*, 1995). For example, previous studies describe a single peri-Rolandic site spread across pre- and postcentral gyri and located contralateral to the stimulated side of the body. Several earlier studies also report bilateral activation of sites along the parietal operculum. One probable factor for differing findings is that current scanners have better spatial resolution, greater tracer sensitivity and higher signal-to-noise ratios. Consequently, we injected lower tracer radioactivity per scan, and yet obtained more scans per subject, thereby further reducing noise by within-subject averaging.

Another likely contributor to the different findings is stimulation protocols. We attempted to nullify completely motor system activity for the hand by using orthopedic casts so that the fingers were held in position for stimulation without effort from the subjects. These techniques also permitted repeated alignment of the grating surfaces against similar distal fingertips within and between subjects. Stimulus parameters were defined better and, despite being suprathreshold, more likely confined to the contact area than in prior studies that stimulated with a massage vibrator (Fox *et al.*, 1987; Seitz and Roland, 1992b; Burton *et al.*, 1993) or that involved unrestrained, self-initiated exploration of object features (Roland, 1993; Ledberg *et al.*, 1995).

Activated Foci in Postcentral Gyrus with Skin Mode Stimulation

An issue is correlating regional blood flow changes with the location of cytoarchitectonic subdivisions across the postcentral gyrus from near the fundus of the central sulcus to, approximately, the fundus of the postcentral sulcus (Brodmann, 1903, 1905; Economo, 1929; Garey, 1994). In our PET images, on the side contralateral to skin mode stimulation, the activated region spares the fundus of the central sulcus, fills the superficial third of the posterior bank of the central sulcus, and covers all of the postcentral gyrus back through the postcentral sulcus. This suggests that blood flow changed across all rather than selected cytoarchitectonic subdivisions. However, inspection of the peaks and distribution of blood flow changes around them suggest possible correlations.

One blood flow peak over the anterior limb of the postcentral gyrus in the skin stimulation mode is probably in area 3b. The relative absence of blood flow changes near the fundus of the central sulcus also suggests sparing of area 3a. The peak occupies the lip; some of the activated region partially extends down along the posterior bank of the central sulcus. Finding activation in presumed area 3b is not surprising since direct stimulation of the skin with embossed gratings mainly stimulates all low threshold mechanoreceptors in contact with the surfaces (Sathian, 1989; Johnson and Hsiao, 1992) and cells in each of the postcentral subdivisions receiving information from these receptors in monkeys (Darian-Smith *et al.*, 1984; Sinclair and Burton, 1991). Cells with receptive fields distant from the fingertips do not respond to these stimuli (Sinclair and Burton, 1991). However, much of the presumed area 3b cortex shows little evidence of blood flow change. This may to some extent reflect averaging across reconstructions in an anatomically highly variable part of cortex (Rademacher *et al.*, 1993; Damasio, 1995).

The second, posterior postcentral activated region is larger and its peak is >1 cm posterior to the anterior focus. The distance between the two peaks is greater than the minimal separable range of the filtered images. The extent of the greatest change in blood flow occupies cortex surrounding the anterior lip of the postcentral sulcus, anterior bank of the postcentral sulcus, and adjoining surface cortex where cytoarchitectonic studies in humans illustrate the border between and neighboring portions of areas 1 and 2. In monkeys the representation for the distal fingertips in area 1 points posterior while in area 2 it is mirror reversed and again points anterior as in area 3b (Pons *et al.*, 1985). There are only a few recordings of responses in area 2 to gratings (Darian-Smith *et al.*, 1984); these responses are consistent with observing information projected from cutaneous receptors to this cortical subdivision (Powell and Mountcastle, 1959; Pons *et al.*, 1985; Iwamura *et al.*, 1993). Assuming an analogous organization, the posterior activated region possibly covers comparable dual finger representations across the border of areas 1 and 2. Thus, the anterior and posterior peaks identified in the PET images might be interpreted as regions activated from multiple distal finger representations: one pointing anterior in area 3b and two joined together at the border between areas 1 and 2.

Previous studies based on different techniques show evidence of multiple somatosensory representations in postcentral, parietal cortex of humans. Recently, we showed with functional magnetic resonance images (fMRI) that rubbing the fingertips with embossed textures activated separate foci within the central and postcentral sulci (Lin *et al.*, 1996). A magneto-encephalography study of the distribution of dipoles evoked by median nerve stimulation (Forss *et al.*, 1994) also illustrated two foci over the postcentral gyrus: one dipole was localized to the central sulcus, possibly area 3b, and another to posterior parietal cortex in the vicinity of the postcentral sulcus (Forss *et al.*, 1994). Woolsey and colleagues recorded positive responses from the surface of the postcentral gyrus while stimulating individual fingers with hard taps (Woolsey *et al.*, 1979). They showed sagittally aligned, 0.5 cm separated points (e.g. Fig. 9 in Woolsey *et al.*, 1979) where stimulating fingers 2/3 evoked responses from sites near the central sulcus and near the anterior lip of the postcentral sulcus. Almost no responses were recorded from the intervening gyral crown. Although not discussed, this remarkable anterior to posterior sequence is suggestive of the two-finger representations later fully described in monkeys. The separation and location of the recordings also agrees with the anterior and posterior peaks observed in the PET images.

Another small focus of increased regional blood flow occupies the same posterior postcentral site ipsilateral to direct skin stimulation. Studies have described cells with bilateral digit tip receptive fields in more posterior parts of the monkey postcentral somatosensory areas (Iwamura *et al.*, 1994); tactile activated ipsilateral sites have also been observed in fMRI (Boecker *et al.*, 1996; Lin *et al.*, 1996). The PET data suggest similar ipsilateral activation with passive tactile stimulation of the fingertips. According to mapping data (Pons *et al.*, 1985) and reconstructions of cortical association connections (Burton and Fabri, 1995), the reported recording sites in monkeys possibly included cutaneous responsive cells in area 2. The ipsilateral posterior site in the PET images directly mirrors the coordinates for the activated focus contralateral to stimulation and, given the

location of the latter (see above), possibly also involves activation of area 2.

Activated Foci in Postcentral Gyrus with Tool Mode Stimulation

The presence of one focus around the posterior limb of the postcentral gyrus with tool mode stimulation suggests possible distinctions between the stimulation modes. Although there are no systematic studies of which peripheral receptors preferentially respond when tools are used to touch objects, inferentially (Johnson and Hsiao, 1992), it is likely sensations from tool mode stimulation predominantly come from non-cutaneous mechanoreceptors because they are sensitive to the low-intensity traveling waves delivered to the finger by perturbations of tools, like plectrums, rubbed against gratings. Possible candidate receptors are Pacinian-like endings in the subdermis, joints and tendons and muscle spindles. Consistent with likely differences in activated receptor populations, subjects reported distinctions in sensations between stimulation modes. For example, gratings were perceived on smooth and rough surfaces only with direct skin contact; the smooth surface was described as completely smooth with the tool mode. The rougher surface felt more like a vibration with the tool. Hence, transitions between the two surfaces were described as more apparent by some subjects with the tool mode. Some subjects localized their sensations to the fingertip with skin mode and to the finger with tool mode.

The features distinguishing tool mode stimulation implicate predominant activation of 'deep' receptor systems. Two findings suggest that the different modes of stimulation may have differentially activated parts of the postcentral gyrus. First, the absence of a separable activation focus near the central sulcus and only a single large posterior focus within the postcentral sulcus are predictable observations from tool mode stimulation when compared to response patterns in monkeys (Powell and Mountcastle, 1959; Jones and Friedman, 1982; Iwamura *et al.*, 1993). Second, finding significantly higher PET difference counts over the anterior postcentral gyrus with skin mode stimulation suggests greater activation in presumed cutaneous dominated parts with direct skin contact. However, these results must be viewed cautiously because the PET activated regions from the two stimulation modes cross-validated each other, indicating that, within the resolution of these techniques, the two regions overlapped.

Foci Activated in Parietal Opercular Cortex

Finding regional blood flow changes in parietal opercular cortex with both modes of stimulation confirms previous reports of this region's importance to somatosensory processes (Penfield and Rasmussen, 1950; Penfield and Jasper, 1954; LaMotte and Mountcastle, 1979; Garcha *et al.*, 1982; Murray and Mishkin, 1984; Roland, 1987; Carlson and Burton, 1988). Previous observations with PET (Talbot *et al.*, 1991; Seitz and Roland, 1992b; Burton *et al.*, 1993; Coghill *et al.*, 1994) identify matched opercular foci in both hemispheres using intense vibratory stimuli. These studies show the greatest changes in regional blood flow on the side contralateral to stimulation. The exclusive contralateral location of activated foci in the present study is consistent with findings in monkeys, where the majority of cells with receptive fields confined to the fingertips respond to stimulation of the contralateral side (Robinson and Burton, 1980a).

Macaque monkeys have two somatosensory maps spread diagonally along the parietal operculum (Burton *et al.*, 1995; Krubitzer *et al.*, 1995). The anterior of these regions receives denser cortical connections from area 3b (Krubitzer *et al.*, 1993; Burton *et al.*, 1995), contains cells with smaller receptive fields, and responds vigorously to stimulation of cutaneous receptors (Robinson and Burton, 1980a). The more posterior S2 region in monkeys receives connections from all postcentral subdivisions, including area 2 (Krubitzer *et al.*, 1993; Burton and Fabri, 1995). Two findings in this study suggest that in humans S2 may also be subdivided. First, the two modes of stimulation activated peaks separated coronally and axially by a posterior-to-medial diagonal distance of ~14 mm. Like the anterior region in monkeys, the peak activated during skin mode stimulation is located nearer the superior limiting sulcus and insula. Similarly, like the posterior S2 region in monkeys, the location of the peak activated during tool mode stimulation lies posterior, superior and closer to the lips of the lateral sulcus in coronal planes posterior to the insula. Second, the average PET difference count from five-pixel diameter voxels centered on the anterior S2 region was significantly higher for skin versus tool mode stimulation. Thus, even though the located foci cross-validated, and therefore the extent of the regions overlapped, there was greater blood flow change over the anterior S2 region with direct skin stimulation.

Ledberg *et al.* (1995) and colleagues also described two foci in the same portion of the parietal operculum. They placed one activated focus on the contralateral side and two sites ipsilateral to the hand used to explore objects for roughness discriminations or to sense taps for a reaction time task. They reported only one ipsilateral site during shape discriminations. The two ipsilateral sites are sagittally separated into a medial one close to the superior limiting sulcus (X = ±45) and, just 2 mm away, a lateral one closer to the lips of the Sylvian fissure (X = ±47). Making distinctions for this distance is a concern as it is less than half the spatial resolution of the PET scanner they used. The two studies show different foci of activation. Our subjects sensed surface roughness with both stimulation modes yet cross-validated foci are entirely contralateral. Ledberg and colleagues reported a more lateral site on the contralateral side only during performance of the roughness discrimination task. The location of this lateral site in their Figure 5*b* visually overlies cortex included in the distribution of our more posterior site. However, this correspondence is largely coincidental because the displayed regions are based on entirely different image transformation methods.

Possible Practice Effects

Regional tracer radioactivity counts were lower in later scans over presumed area 3b and the parietal operculum in humans making repeated roughness estimates. Such decreases in averaged PET counts with time imply less activity and possibly a more restricted region of cortex activated from the stimulated skin. This is contrary to evidence of increased representations in recordings from area 3b of normal monkeys upon repetitious use of one or more fingers in tactile discrimination tasks (Recanzone *et al.*, 1992; Wang *et al.*, 1995). However, the direction of these changes may be time dependent. Karni *et al.* (1995) showed, with fMRI measurements, decreases in activated area of primary motor cortex only after initial habituation followed by increases with extended weekly training. Thus, finding decreases in PET counts after three or more scans involving roughness estimates of the same surfaces may reflect habituation effects. However, this explanation does not account for the increased activation

bilaterally in the region associated with the posterior limb of the postcentral gyrus in the same subjects. These magnitude shifts in activation suggest that habituation may also involve changes in which areas of cortex process incoming stimuli (Raichle *et al.*, 1994). The studies describing expanded representations only report changes in area 3b. Finding an opposite direction of change in the PET images between anterior and posterior zones, and given that these two appear to coincide with separate subdivisions of S1 in humans, suggests that potentially different plasticity effects might occur in different S1 subdivisions.

Shifts in activation foci to different brain regions have previously been observed when subjects become practiced in verb generate tasks (Raichle *et al.*, 1994). The present results show that the magnitude of activation changes with habituation. These findings (and several other studies cited in Raichle *et al.*, 1994) suggest that initial experience with novel events may involve different cortical areas than those used for learned, more automatic processing. A possibility is the role of different cortical regions in extracting, analyzing and transforming stimulus features. Thus, anterior postcentral gyrus regions and S2 might encode multiple parameters of surface roughness and posterior postcentral gyrus regions respond to encrypted, more abstract aspects of surface texture.

Foci Activated in Frontal Cortex

The focus on the middle frontal gyri corresponds to a portion of premotor area 6 that in monkeys has some cells activated by passive tactile stimuli but larger responses when these stimuli trigger a learned motor response (Kurata and Tanji, 1986). Tactile stimulus activation of the supplementary motor area (e.g. our medial frontal gyrus site) is also greater when monkeys do behavioral tasks conditioned to tactile stimuli (Romo *et al.*, 1993). The presence of these frontal cortex activations is not just because stimulation conditionally couples to motor responses. Our subjects integrated tactile sensations, judged roughness, stored this estimation until the scan was over, and then reported their sensation magnitudes. Stimulus-triggered motor acts involve integration of selected stimulus features leading to stored associations with particular motor acts. The aspect common to these tasks is sensory integration preceding some response. This suggests that premotor cortex may play a role in setting 'motor responses' based on previewing and integrating sensory information projected to it from sensory areas of the brain. According to this hypothesis, premotor cortex activation occurs for any task that requires sensory judgements leading to potentially different responses.

The absence of blood flow changes in primary motor cortex (e.g. precentral gyrus site) during skin mode stimulation differs appreciably from previous reports (Fox *et al.*, 1987; Seitz and Roland, 1992a; Ledberg *et al.*, 1995). This difference may reflect our experimental procedures. There was minimal use of the motor system for holding the hand in position for stimulation and our subjects did not actively explore objects. Stimulus intensities were low and possibly only activated reflex contractions in the intrinsic hand muscles during tool mode stimulation. The latter potentially accounts for the small peak over the precentral gyrus with tool mode stimulation. However, if these contractions occurred, the absence of blood flow changes near area 3a is puzzling, i.e. from muscle spindle activation needed to create the reflex contractions.

Notes

Special thanks to Len Lich, John Hood and the staff of the Cyclotron Unit for technical assistance, Tom Yang and Avi Synder for algorithms used in image reconstructions, Fred Kuhns for computer maintenance and network management, John Kreitler for design and construction of the stimulator, and Robert Sinclair for statistics consultations. This work was supported by NIH Grants NS 31005, HL 13851 and NS 06833 and funds from the McDonnell Center for the Study of Higher Brain Function.

Address correspondence to: Dr H. Burton, Department of Anatomy and Neurobiology, Washington University School of Medicine, 660 South Euclid Avenue, St Louis, MO 63110, USA.

References

Baumgartner C, Doppelbauer A, Deecke L, Barth DS, Zeitlhofer J, Lindinger G, Sutherling WW (1991) Neuromagnetic investigation of somatotopy of human hand somatosensory cortex. Exp Brain Res 87:641–648.

Boecker H, Khorram-Sefat D, Kleinschmidt A, Merboldt K-D, Hänicke W, Requardt M, Frahm J (1996) High-resolution functional magnetic resonance imaging of cortical activation during tactile exploration. Hum Brain Map 3:236–244.

Brodmann K (1903) Beiträge zur histologischen Lokalisation der Grosshirnrinde. I. Mitt. Die Regio Rolandica. J Psychol Neurol 2:79–107.

Brodmann K (1905) Beiträge zur histologischen Lokalisation der Grosshirnrinde. III. Mitt. Die Rindenfelder der niederen Affen. J Psychol Neurol 4:177–226.

Burton H (1986) Second somatosensory cortex and related areas. In: Cerebral cortex, sensory-motor areas and aspects of cortical connectivity (Jones EG, Peters A, eds), pp 31–98. New York: Plenum.

Burton H, Fabri M (1995) Ipsilateral intracortical connections of physiologically defined cutaneous representations in areas 3b and 1 of macaque monkeys: projections in the vicinity of the central sulcus. J Comp Neurol 355:508–538.

Burton H, Fabri M, Alloway K (1995) Cortical areas within the lateral sulcus connected to cutaneous representations in areas 3b and 1: a revised interpretation of the second somatosensory area in macaque monkeys. J Comp Neurol 355:539–562.

Burton H, Videen TO, Raichle ME (1993) Tactile vibration activated foci in insular and parietal opercular cortex studied with positron emission tomography: mapping the second somatosensory area in humans. Somatosens Mot Res 10:297–308.

Campbell AW (1905) Histological studies on the localization of cerebral function. London: Cambridge University Press.

Carlson M, Burton H (1988) Recovery of tactile function after damage to primary or secondary somatic sensory cortex in infant macaca mulatta. J Neurosci 8:833–859.

Casey KL, Minoshima S, Berger KL, Koeppe RA, Morrow TJ, Frey KA (1994) Positron emission tomography analysis of cerebral structures activated specifically by repetitive noxious heat stimuli. J Neurophysiol 71:802–807.

Coghill RC, Talbot JD, Evan AC, Meyer E, Gjedde A, Bushnell MC, Duncan GH (1994) Distributed processing of pain and vibration by the human brain. J Neurosci 14:4095–4108.

Damasio H (1995) Human brain anatomy in computerized images. New York: Oxford University Press.

Darian-Smith I, Goodwin A, Sugitani M, Heywood J (1984) The tangible features of textured surfaces: Their representation in the monkey's somatosensory cortex. In: dynamic aspects of neocortical function (Edelman GM, Gall WE, Cowan WM, eds), pp 475–500. New York: Wiley.

Drevets WC, Burton H, Videen TO, Snyder AZ, Simpson J J.R., Raichle ME (1995) Blood flow changes in human somatosensory cortex during anticipated stimulation. Nature 373:249–252.

Economo Cv (1929) The cytoarchitectonics of the human cerebral cortex. London: Oxford University Press.

Forss N, Hari R, Salmelin R, Ahonen A, Hamalainen M, Kajola M, Knuutila J, Simola J (1994) Activation of the human posterior parietal cortex by median nerve stimulation. Exp Brain Res 99:309–15.

Fox PT, Burton H, Raichle ME (1987) Mapping human somatosensory cortex with positron emission tomography. J Neurosurg 67:34–43.

Fox PT, Mintun MA (1989) Noninvasive functional brain mapping by change-distribution analysis of averaged PET images of $H_2{}^{15}O$ tissue activity. J Nucl Med 30:141–149.

Fox PT, Mintun MA, Raichle ME, Herscovitch P (1984) A noninvasive approach to quantitative functional brain mapping with $H_2{}^{15}O$ and positron emission tomography. J Cereb Blood Flow 4:329–333.

Fox PT, Mintun MA, Reiman EM, Raichle ME (1988) Enhanced detection of focal brain responses using intersubject averaging and change-distribution analysis of subtracted PET images. J Cereb Blood Flow 8:642–653.

Fox PT, Perlmutter JS, Raichle ME (1985) A stereotactic method of anatomical localization for positron emission tomography. J Comput Assist Tomogr 9:141–153.

Garcha HS, Ettlinger G, Maccabe JJ (1982) Unilateral removal of the second somatosensory projection cortex in the monkey: evidence for cerebral predominance? Brain 105:787–810.

Garey LJ (1994) Brodmann's 'Localisation in the cerebral cortex'. London: Smith-Gordon.

Hammeke TA, Yetkin FZ, Mueller WM, Morris GL, Haughton VM, Rao SM, Binder JR (1994) Functional magnetic resonance imaging of somatosensory stimulation. Neurosurgery 35:677–81.

Hari R, Hamalainen M, Kaukoranta E, Reinikainen K, Teszner D (1983) Neuromagnetic responses from the second somatosensory cortex in man. Acta Neurol Scand 68:207–12.

Hari R, Karhu J, Hamalainen M, Knuutila J, Salonen O, Sams M, Vilkman V (1993) Functional organization of the human first and second cortices: a neuromagnetic study. Eur J Neurosci 5:724–734.

Houton DL, Miezin FM, Buckner RL, vanMier HI, Raichle ME, Petersen SE (1996) An assessment of functional anatomical variability in neuroimaging studies. Hum Brain Map (in Press).

Hyvärinen J (1982) Posterior parietal lobe of the primate brain. Physiol Rev 62:1060–1129.

Iwamura Y, Iriki A, Tanaka M (1994) Bilateral hand representation in the postcentral somatosensory cortex. Nature 369:554–556.

Iwamura Y, Tanaka M, Sakamoto M, Hikosaka O (1993) Rostrocaudal gradients in the neuronal receptive field complexity in the finger region of the alert monkey's postcentral gyrus. Exp Brain Res 92:360–368.

Johnson KO, Hsiao SS (1992) Neural mechanisms of tactual form and texture perception. Annu Rev Neurosci 15:277–350.

Jones EG (1985) The thalamus. New York: Plenum.

Jones EG, Friedman DP (1982) Projection patterns of functional components of thalamic ventrobasal complex on monkey somatosensory cortex. J Neurophysiol 48:521–544.

Jones EG, Porter R (1980) What is area 3a? Brain Res Rev 2:1–43.

Jones EG, Powell TPS (1970) An anatomical study of converging sensory pathways within the cerebral cortex of the monkey. Brain 93:793–820.

Kaas JH, Nelson RJ, Sur M, Lin C-S, Merzenich MM (1979) Multiple representations of the body within the primary somatosensory cortex of primates. Science 204:521–523.

Karni A, Meyer G, Jezzard P, Adams MM, Turner R, Ungerleider LG (1995) Functional MRI evidence for adult motor cortex plasticity during motor skill learning. Nature 377:155–158.

Keppel G (1982) Design and analysis: a researcher's handbook. Englewood Cliffs, NJ: Prentice Hall.

Krubitzer L, Clarey J, Tweedale R, Elston G, Calford M (1995) A redefinition of somatosensory areas in the lateral sulcus of macaque monkeys. J Neurosci 15:3821–3839.

Krubitzer LA, Calford MB, Schmid LM (1993) Connections of somatosensory cortex in megachiropteran bats: the evolution of cortical fields in mammals. J Comp Neurol 327:473–506.

Kurata K, Tanji J (1986) Premotor cortex neurons in macaques: activity before distal and proximal forelimb movements. J Neurosci 6:403–411.

LaMotte RH, Mountcastle VB (1979) Disorders in somesthesis following lesions of parietal lobe. J Neurophysiol 42:400–419.

Ledberg A, O'Sullivan BT, Kinomura S, Roland PE (1995) Somatosensory activations of the parietal operculum of man. A PET study. Eur J Neurosci 7:1934–1941.

Lin W, Kuppusamy K, Haacke EM, Burton H (1996) Functional magnetic resonance imaging in human somatosensory cortex activated by touching textured surfaces. J Mag Res Imag 6:565–572.

Mintun MA, Fox PT, Raichle ME (1989) A highly accurate method of localizing regions of neuronal activation in the human brain with positron emission tomography. J Cereb Blood Flow 9:96–103.

Mogilner A, Nomura M, Ribary U, Jagow R, Lado F, Rusinek H, Llinas R (1994) Neuromagnetic studies of the lip area of primary somatosensory cortex in humans: evidence for an oscillotopic organization. Exp Brain Res 99:137–47.

Murray EA, Mishkin M (1984) Relative contributions of SmII and area 5 to tactile discrimination of monkeys. Behav Brain Res 11:67–84.

Nelson RJ, Sur M, Felleman DJ, Kaas JH (1980) Representations of the body surface in postcentral parietal cortex of *Macaca fascicularis*. J Comp Neurol 192:611–643.

Okada YC, Tanenbaum R, Williamson SJ, Kaufman L (1984) Somatotopic organization of the human somatosensory cortex revealed by neuromagnetic measurements. Exp Brain Res 56:197–205.

Paul RL, Merzenich M, Goodman H (1972) Representation of slowly and rapidly adapting cutaneous mechanoreceptors of the hand in Brodman's areas 3 and 1 of *Macaca mulatta*. Brain Res 36:229–249.

Penfield W, Jasper H (1954) Epilepsy and the functional anatomy of the human brain. London: Churchill.

Penfield W, Rasmussen T (1950) Secondary sensory and motor representation. New York: Macmillan.

Pons TP, Garraghty PE, Cusick CG, Kaas JH (1985) The somatotopic organization of area 2 in macaque monkeys. J Comp Neurol 241:445–466.

Pons TP, Wall JT, Garraghty PE, Cusick CG, Kaas JH (1987) Consistent features of the representation of the hand in area 3b of macaque monkeys. Somatosens Res 4:309–331.

Powell TPS, Mountcastle VB (1959) Some aspects of the functional organization of the cortex of the postcentral gyrus of the monkey: a correlation of findings obtained in a single unit analysis with cytoarchitecture. Bull Johns Hopkins Hosp 105:133–162.

Puce A, Constable RT, Luby ML, McCarthy G, Nobre AC, Spencer DD, Gore JC, Allison T (1995) Functional magnetic resonance imaging of sensory and motor comparison with electrophysiological localization. J Neurosurg 83:262–70.

Raczkowski D, Kalat JW, Nebes R (1974) Reliability and validity of some handedness questionnaire items. Neuropsychologia 6:43–47.

Rademacher J, Caviness J V.S., Steinmetz H, Galaburda AM (1993) Topographical variation of the human primary cortices: Implications for neuroimaging, brain mapping, and neurobiology. Cereb Cortex 3:313–329.

Raichle ME, Fiez JA, Videen TO, Pardo JV, Fox PT, Petersen SE (1994) Practice-related changes in human brain functional anatomy during nonmotor learning. Cereb Cortex 4:8–26.

Recanzone GH, Merzenich MM, Jenkins WM, Grajski KA, Dinse HR (1992) Topographic reorganization of the hand representation in cortical area 3b of owl monkeys trained in a frequency-discrimination task. J Neurophysiol 67:1031–1056.

Robinson CJ, Burton H (1980a) Somatotopographic organization in the second somatosensory area of *M. fascicularis*. J Comp Neurol 192:43–67.

Robinson CJ, Burton H (1980b) Organization of somatosensory receptive fields in cortical areas 7b, retroinsula, postauditory and granular insula of *M. fascicularis*. J Comp Neurol 192:69–92.

Robinson CJ, Burton H (1980c) Somatic submodality distribution within the second somatosensory (SII), 7b, retroinsular, postauditory, and granular insular cortical areas of M. fascicularis. J Comp Neurol 192:93–108.

Roland PE (1987) Somatosensory detection of miocrogeometry, macrogeometry and kinesthesia after localized lesions of the cerebral hemispheres in man. Brain Res Rev 12:43–94.

Roland PE (1993) Brain activation. New York: Wiley-Liss.

Roland PE, Seitz RJ (1991) Positron emission tomography studies of the somatosensory system in man. Ciba Foundation Symposium 163:113–120.

Romo R, Ruiz S, Crespo P, Zainos A, Merchant H (1993) Representation of tactile signals in primate supplementary motor area. J Neurophysiol 70:2690–2694.

Sathian K (1989) Tactile sensing of surface features. Trends Neurosci 12:513–519.

Seitz RJ, Roland PE (1992a) Variability of the regional cerebral blood flow pattern studied with [11C]-fluoromethane and position emission tomography (PET). Comput Med Imag Graph 16:311–22.

Seitz RJ, Roland PE (1992b) Vibratory stimulation increases and decreases the regional cerebral blood flow and oxidative metabolism: a positron emission tomography (PET) study. Acta Neurol Scand 86:60–7.

Sinclair RJ, Burton H (1991) Neuronal activity in the primary somatosensory cortex in monkeys (*Macaca mulatta*) during active touch of textured surface gratings: responses to groove width, applied force and velocity of motion. J Neurophysiol 66:153–169.

Squire LR, Ojemann JG, Miezin FM, Petersen SE, Videen TO, Raichle ME (1992) Activation of the hippocampus in normal humans: a functional anatomical study of memory. Proc Natl Acad Sci USA 89:1837–1841.

Suk J, Ribary U, Cappell J, Yamamoto T, Llinas R (1991) Anatomical localization revealed by MEG recordings of the somatosensory system. Electroencephalogr Clin Neurophysiol 78:185–96.

Talairach J, Tournoux P (1988) Co-planar stereotaxic atlas of the human brain. Stuttgart: Thieme.

Talbot JD, Marrett S, Evans AC, Meyer E, Bushnell MC, Duncan GH (1991) Multiple representations of pain in human cerebral cortex. Science 251:1355–1358.

Wang X, Merzenich MM, Sameshima K, Jenkins WM (1995) Remodelling of hand representation in adult cortex determined by timing of tactile stimulation. Nature 378:71–75.

Woolsey CN, Erickson TC, Gilson WE (1979) Localization in somatic sensory and motor areas of human cerebral cortex as determined by direct recording of evoked potentials and electrical stimulation. J Neurosurg 51:476–506.